

Supplementary Materials for

Approaching the forbidden fruit of reaction dynamics: Aiming reagent at selected impact parameters

Kelvin Anggara, Lydie Leung, Matthew J. Timm, Zhixin Hu, John C. Polanyi*

*Corresponding author. Email: jpolanyi@chem.utoronto.ca

Published 5 October 2018, *Sci. Adv.* **4**, eaau2821 (2018)

DOI: 10.1126/sciadv.aau2821

The PDF file includes:

Supplementary Text

Fig. S1. Computed dynamics for the electron-induced reaction of CF_3 , obtained from the I2S model.

Fig. S2. Distance dependence of the energy in the recoiling CF_2 .

Fig. S3. Identification of molecular species on the surface.

Fig. S4. $\text{CF}_2 + \text{I}$ collision at 1.80 Å impact parameter, giving only momentum transfer from the projectile to the target.

Fig. S5. Nonreactive outcome of a zero-impact parameter $\text{CF}_2 + \text{CF}_2$ collision, resulting in only momentum transfer from the projectile to the target.

Fig. S6. Trajectory for direct association reaction superimposed on a restricted cut through the ground potential energy surface.

Fig. S7. Trajectory for indirect association reaction superimposed on a restricted cut through the ground potential energy surface.

Fig. S8. Evidence for electron-induced reaction.

Legends for movies S1 to S3

Other Supplementary Material for this manuscript includes the following:

(available at advances.sciencemag.org/cgi/content/full/4/10/eaau2821/DC1)

Movie S1 (.mp4 format). Computed dynamics for the electron-induced reaction of CF_3 , obtained from the I2S model.

Movie S2 (.mp4 format). Computed dynamics for direct reaction.

Movie S3 (.mp4 format). Computed dynamics for indirect reaction.

Supplementary Text

Mechanism of electron-induced reaction

The electron-induced dissociation of CF_3 exhibited an onset threshold-energy of ~ 0.9 eV. This threshold is in satisfactory agreement with the results of a density-of-states calculation of chemisorbed CF_3 (see fig. S8A) which shows a $\text{CF}_3\text{-Cu}$ hybrid state at 1.3 eV with an onset at ~ 0.7 eV. The charge density in this hybrid state exhibited anti-bonding character in the C-F bond, consistent with the observed C-F bond-breaking. The electron-induced dissociation of CF_3 was found to be a single electron process as evidenced by the linear relationship between the reaction rate and the tunneling current (see fig. S8B). Hence the CF_3 dissociation can be understood to proceed via electronic excitation by a single electron, modeled here using the Impulsive Two-State model (see Methods).

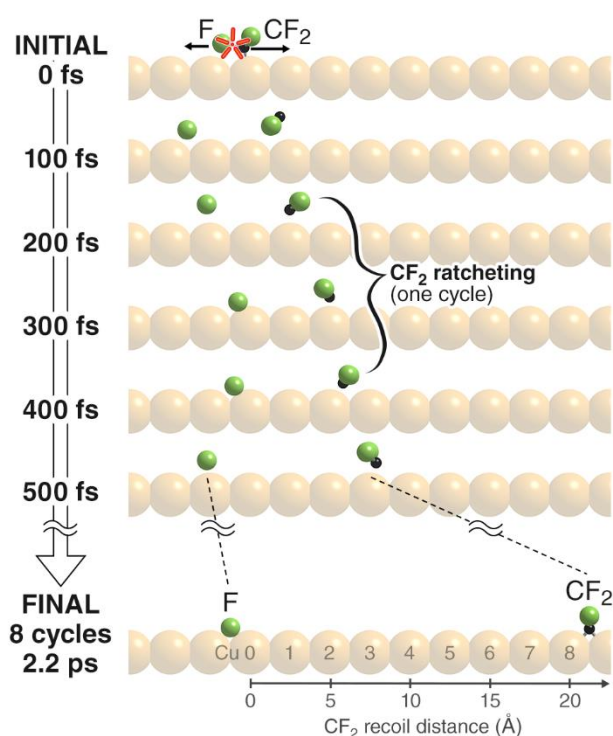


Fig. S1. Computed dynamics for the electron-induced reaction of CF_3 , obtained from the I2S model. The trajectory was obtained by placing an electron in the F-atom of the C-F bond directed along the Cu-row for a $t^* = 13$ fs (see also movie S1). The impulse (red explosion at $t = 0$ fs) propelled the F-atom and the CF_2 in opposite directions. The CF_2 ‘ratcheted’ for 8 unit cells before stopping at 8.5 unit cells away (21.7 \AA) from its initial position. The trajectory reproduced the average recoil distance of the CF_2 observed in the experiment (19.7 \AA).

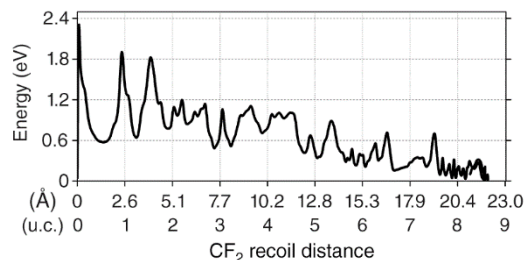


Fig. S2. Distance dependence of the energy in the recoiling CF_2 . The energy shown is the sum of the translational and rotational energies of CF_2 in the I2S trajectory shown in fig. S1 and movie S1.

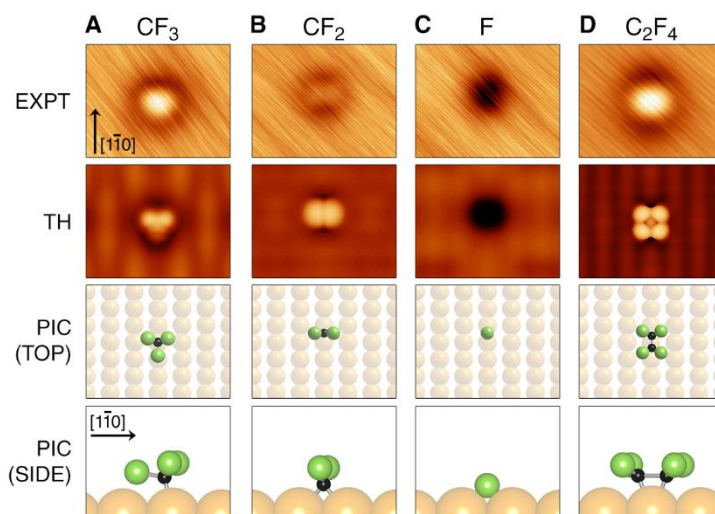


Fig. S3. Identification of molecular species on the surface. STM images (EXPT), STM simulations (TH) and molecular models (PIC) are given for a chemisorbed (A) trifluoromethyl (CF_3), (B) difluorocarbene (CF_2), (C) fluorine atom, and (D) tetrafluoroethylene (C_2F_4). The imaged CF_3 was 0.07 ± 0.04 nm in height, the CF_2 was 0.23 ± 0.04 nm in depth, the F-atom was 0.36 ± 0.04 nm in depth and the C_2F_4 was 0.29 ± 0.04 nm in height.

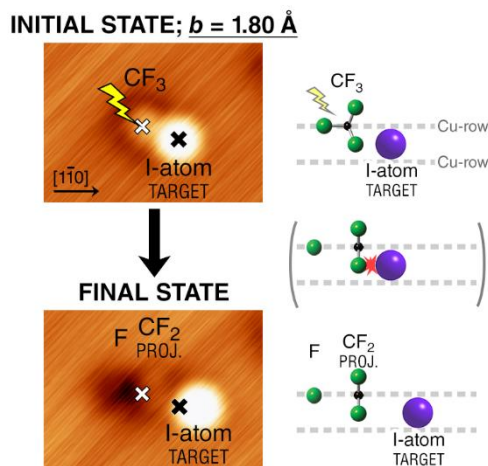


Fig. S4. $\text{CF}_2 + \text{I}$ collision at 1.80 \AA impact parameter, giving only momentum transfer from the projectile to the target. STM images and schematics showing the initial and final state of

the 1.80 Å impact parameter collision between the CF₂ projectile and the I-atom target. The collision caused the I-atom target to be displaced along the continuation of the approach direction of the CF₂ projectile. The tip was placed above the CF₃ (white cross) to produce the CF₂ projectile. The black cross marks the initial position of the I-atom target.

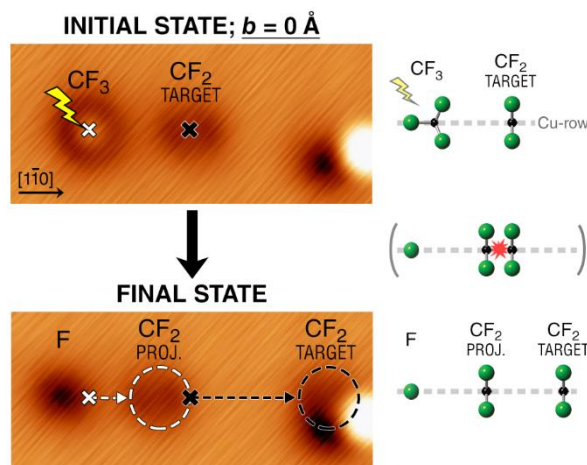


Fig. S5. Nonreactive outcome of a zero-impact parameter CF₂ + CF₂ collision, resulting in only momentum transfer from the projectile to the target. STM images and schematics showing the initial and final state of the zero impact parameter collision. The collision caused the CF₂ target to be displaced along the approach direction of the CF₂ projectile. The tip was placed above the CF₃ (white cross) to produce the CF₂ projectile. The black cross marks the initial position of the CF₂ target. In the final state, the new position of CF₂ projectile is marked by white dashed circle, and that of the CF₂ target is marked by a black dashed circle.

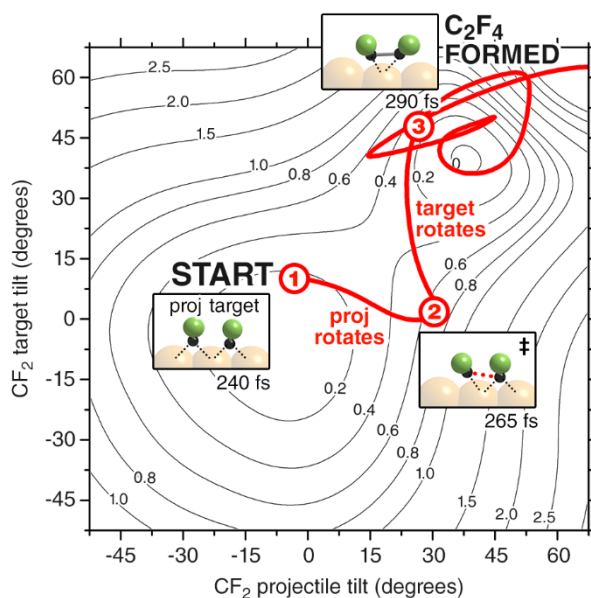


Fig. S6. Trajectory for direct association reaction superimposed on a restricted cut through the ground potential energy surface. The cut was obtained by calculating the potential energy of independently rotated CF₂ projectile and CF₂ target, while the distance between the two CF₂

was kept constant at their closest approach (2.55 \AA , 1 unit cell). The red line shows the superimposed trajectory for Direct reaction, shown in Fig. 4A of the main text, obtained by MD calculations employing the full potential-energy surface for 126 atoms. The inset shows the nuclear positions of the system at different times in the trajectory, with both CF_2 at their closest distance of approach at 240 fs in Panel 1, at the transition state located at 265 fs in Panel 2, and for C_2F_4 product at 290 fs in Panel 3. The dotted black lines in all Panels indicate the C-Cu bond. The dotted red-line in Panel 2 indicates attraction at the inception of C-C bond formation, evidenced by the negative slope of the potential towards the C_2F_4 product potential well in the transition state at 265 fs. The dynamics in Direct Association shows a stepwise process in which (i) the rotation of the projectile towards the target is followed by (ii) the rotation of the target towards the projectile, thereby forming a C-C bond.

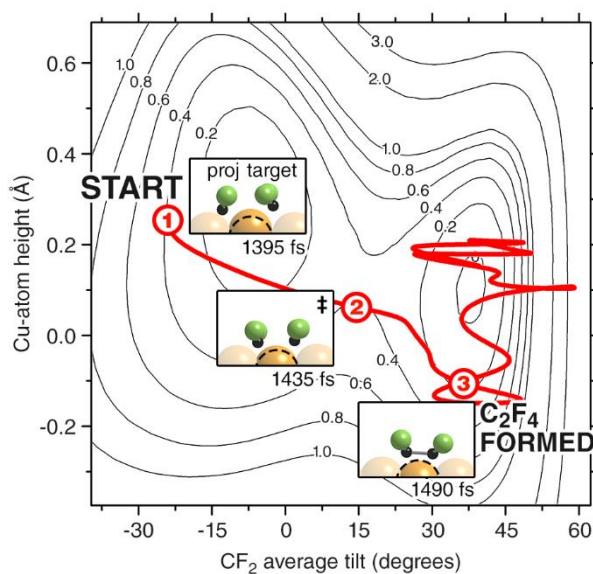


Fig. S7. Trajectory for indirect association reaction superimposed on a restricted cut through the ground potential energy surface. The cut was obtained by calculating the potential energy of both CF_2 rotated in tandem at various Cu-atom heights, while the distance between the two CF_2 was kept constant at their closest approach (2.55 \AA , 1 unit cell). The red line shows the superimposed trajectory for Indirect reaction, shown in Fig. 4B of the main text, obtained by MD calculations employing the full potential-energy surface for 126 atoms. The inset shows the nuclear positions of the system at different times in the trajectory, showing both CF_2 in their closest approach distance at 1395 fs in Panel 1, the transition state at 1435 fs in Panel 2, and the C_2F_4 product at 1490 fs in Panel 3. The black dashed circle indicates the position of an un-raised Cu-atom. The dynamics in Indirect Association shows that the C-C bond formation is assisted by the raised Cu-atom.

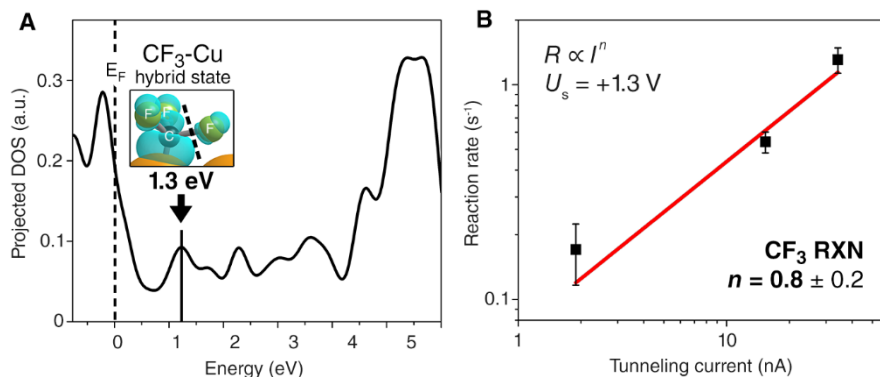


Fig. S8. Evidence for electron-induced reaction. (A) Computed projected density-of-states for a chemisorbed CF_3 on $\text{Cu}(110)$. The inset shows the real-space visualization (isocontour: $0.00015 \text{ e}^- \text{ \AA}^{-3}$) of the CF_3 -Cu hybrid state centered at 1.3 eV. The nodal plane given by the dashed line between C- and F-atom indicates C-F σ^* anti-bonding character. (B) A log-log plot of the reaction rate against the tunneling current at +1.3 V bias obtained from experiment. Linear fit of the data gives $n = 0.8 \pm 0.2$ as the slope, indicative of a one-electron process. The error bar on each data point corresponds to the standard error in the fitting of the exponential function to the data (see Methods for details).

Movie S1. Computed dynamics for the electron-induced reaction of CF_3 , obtained from the I2S model. The trajectory was obtained by placing an electron in the F-atom of the C-F bond directed along the Cu-row for a $t^* = 13$ fs. The frame rate for movie playback is 24 fps where each frame has 3 fs duration.

Movie S2. Computed dynamics for direct reaction. The trajectory was obtained by placing a stationary CF_2 target in the path of the recoiling CF_2 projectile from movie S1 at 179 fs. The target was placed 3.5 unit cells (8.93 \AA) away from the CF_3 (i.e. away from the parent molecule of the CF_2 projectile). The frame rate for movie playback is 24 fps where each frame has 3 fs duration. [The phantom bonds at the 15-second to 19-second marks were caused by the molecule crossing the boundary of a periodic supercell.]

Movie S3. Computed dynamics for indirect reaction. The trajectory was obtained by placing a stationary CF_2 target in the path of the recoiling CF_2 projectile from movie S1 at 179 fs. The target was placed 4.5 unit cells (11.47 \AA) away from the CF_3 (the parent molecule of the CF_2 projectile). The frame rate for movie playback is 24 fps where each frame has 3 fs duration.